



Published in final edited form as:

*Pharmacol Res.* 2017 May ; 119: 89–98. doi:10.1016/j.phrs.2017.01.024.

## Modulating the function of ATP-binding cassette subfamily G member 2 (ABCG2) inhibitor cabozantinib

Guan-Nan Zhang<sup>1</sup>, Yun-Kai Zhang<sup>1</sup>, Yi-Jun Wang<sup>1</sup>, Anna Maria Barbuti<sup>1</sup>, Xi-Jun Zhu<sup>1,2,#</sup>, Xin-Yue Yu<sup>1,3,#</sup>, Ai-Wen Wen<sup>1,4,#</sup>, John N.D. Wurpel<sup>1</sup>, and Zhe-Sheng Chen<sup>1,\*</sup>

<sup>1</sup>Department of Pharmaceutical Sciences, College of Pharmacy and Health Sciences, St. John's University, Queens, New York 11439, USA

<sup>2</sup>The Affiliated High School of South China Normal University, Guangzhou, Guangdong, 510630, China

<sup>3</sup>Zhixin High School, Guangzhou, Guangdong, 510000, China

<sup>4</sup>Guangdong Pharmaceutical University, Guangzhou, Guangdong, 510515, China

### Abstract

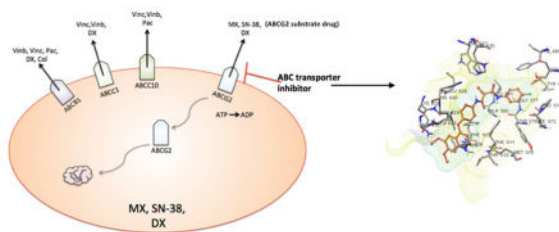
Cabozantinib (XL184) is a small molecule tyrosine kinase receptor inhibitor, which targets c-Met and VEGFR2. Cabozantinib has been approved by the Food and Drug Administration to treat advanced medullary thyroid cancer and renal cell carcinoma. In the present study, we evaluated the ability of cabozantinib to modulate the function of the ATP-binding cassette subfamily G member 2 (ABCG2) by sensitizing cells that are resistant to ABCG2 substrate antineoplastic drugs. We used a drug-selected resistant cell line H460/MX20 and three ABCG2 stable transfected cell lines ABCG2-482-R2, ABCG2-482-G2, and ABCG2-482-T7, which overexpress ABCG2. Cabozantinib, at non-toxic concentrations (3 or 5  $\mu$ M), sensitized the ABCG2-overexpressing cells to mitoxantrone, SN-38, and topotecan. Our results indicate that cabozantinib reverses ABCG2-mediated multidrug resistance by antagonizing the drug efflux function of the ABCG2 transporter instead of downregulating its expression. The molecular docking analysis indicates that cabozantinib binds to the drug-binding site of the ABCG2 transporter. Overall, our findings demonstrate that cabozantinib inhibits the ABCG2 transporter function and consequently enhances the effect of the antineoplastic agents that are substrates of ABCG2. Cabozantinib may be a useful agent in anticancer treatment regimens for patients who are resistant to ABCG2 substrate drugs.

### Graphical abstract

\* Author for Correspondence: Zhe-Sheng Chen, M.D. Ph.D., Department of Pharmaceutical Sciences, St. John's University, Queens, New York, 11439, USA. chenz@stjohns.edu, Phone: 1-718-990-1432.

# Xi-Jun Zhu, Xin-Yue Yu and Ai-Wen Wen are the summer students at St. John's University.

**Publisher's Disclaimer:** This is a PDF file of an unedited manuscript that has been accepted for publication. As a service to our customers we are providing this early version of the manuscript. The manuscript will undergo copyediting, typesetting, and review of the resulting proof before it is published in its final citable form. Please note that during the production process errors may be discovered which could affect the content, and all legal disclaimers that apply to the journal pertain.



## Keywords

Cabozantinib; Breast cancer resistant protein; Multidrug resistance; ABC transporter

## 1. Introduction

Multidrug resistance (MDR) is one of the major mechanisms responsible for chemotherapeutic failure. MDR is a phenomenon of cancer cells developing resistance to several mechanistically and structurally unrelated antineoplastic drugs [1,2]. Overexpression of ATP binding cassette (ABC) transporters is regarded as one of the major mechanisms of MDR; this leads to increased drug efflux which significantly reduces the intracellular concentration of antineoplastic agents [2,3]. Currently, 48 human ABC transporters have been identified and characterized. ABCB1, or P-glycoprotein (P-gp), was the first to be identified, encoded by the *MDR1* gene [3]. ABCG2 is the second member of subfamily G of the ABC transporters, and is also known as breast cancer resistance protein (BCRP) [4,5]. Unlike ABCB1, which consists of two transmembrane domains (TMDs) and two nucleotide-binding domains (NBDs), ABCG2 is a half-transporter, which has only one NBD and one TMD [6]. Overexpression of the ABCG2 protein is responsible for high levels of resistance to a variety of antineoplastic drugs, including mitoxantrone (MX), anthracycline, topotecan, irinotecan and SN-38 [5,7–11]. It has been demonstrated that overexpression of ABCG2 is responsible for MDR, due to its ability to pump out the substrate anticancer drugs and thus decreasing intracellular concentration of drugs [4,12,13]. Reversing MDR by administering ABCG2 protein inhibitors concurrently with ABCG2 substrate antineoplastic drugs is regarded as a potential pharmacological approach to effective cancer treatment [14–16]. A limited number of ABCG2 inhibitors demonstrate the ability to sensitize drug resistant cells to substrate antineoplastic drugs. Some excellent ABCB1 inhibitors have been found to function as inhibitors of ABCG2 [17–19]. For example, the potent P-gp inhibitor GF120918 is effective in reversing ABCG2 transporter induced MDR, with an  $IC_{50}$  value of 50 nM [20]. Potent dual ABCB1/ABCG2 inhibitors also include tyrosine kinase inhibitors such as imatinib, bafetinib, and nilotinib [17,21,22].

Cabozantinib (XL184) is a tyrosine kinase inhibitor targeting c-Met as well as vascular endothelial growth factor receptor 2 (VEGFR2), which are both dysregulated in various types of cancer [23,24]. On April 25, 2016, cabozantinib was approved by the FDA for the treatment of advanced renal cell carcinoma. Additionally, it has been approved to treat advanced medullary thyroid cancer, and is also being investigated in clinical trials to treat other solid tumors, including renal, prostate, ovarian, and breast cancer [24–28]. The

structure of cabozantinib is shown in Fig 1. In a preclinical study, a lower concentration of cabozantinib was used to inhibit the phosphorylation of HGFR and VEGFR2 in different cancer cell lines [24]. Several phase II studies are being carried out to employ cabozantinib in the treatment of advanced carcinoid and pancreatic neuroendocrine tumors, non-small cell lung cancer, breast cancer, and hepatocellular carcinoma [25,27,29–31]. Patients were given 60 mg of cabozantinib orally per day for the treatment of renal cell carcinoma and non-small-cell lung cancer, and 140 mg per day for the treatment of metastatic medullary thyroid carcinoma [32]. In the present study, we investigate the effect of cabozantinib as a therapeutic compound to increase the chemo-sensitivity of conventional anticancer drugs through its interaction with the ABCG2 transporter.

## 2. Materials and methods

### 2.1 Chemicals

[<sup>3</sup>H]-MX (4Ci/mmol) was purchased from Moravек Biochemicals, Inc. (Brea, CA). Tween20, NaCl, Tris-HCl, sodium dodecyl sulphate (SDS), Triton X-100, dimethyl sulfoxide (DMSO), 3-(4,5-dimethylthiazol-2-yl)-2,5-diphenyltetrazolium bromide (MTT), penicillin/streptomycin, topotecan, SN-38, and MX were purchased from Sigma-Aldrich (St. Louis, MO). Cabozantinib was generously provided by ChemiTex (Brussels Belgique). Fumitremogin C (FTC) was kindly synthesized by Thomas McCloud, Developmental Therapeutics Program, Natural Products Extraction Laboratory, NCI, NIH (Bethesda, MD). The ABCG2 monoclonal antibody BXP-21 (GTX23380) was purchased from GeneTex (Irvine, CA). The anti-actin monoclonal antibody (sc-8432) was purchased from Santa Cruz Biotechnology, Inc. (Santa Cruz, CA). Dulbecco modified Eagle medium (DMEM), fetal bovine serum (FBS), phosphate buffer saline (PBS), and trypsin 0.25% EDTA were purchased from Hyclone (Waltham, MA). Ammonium molybdate, MES hydrate, antimony potassium tartrate, sodium azide and N-methyl-D-glucamine were purchased from Sigma-Aldrich (St. Louis, MO). Potassium phosphate, EGTA and ATP were products of AMRESCO (Solon, OH). Sulfuric acid solution (37N) was purchased from Fisher Scientific (Pittsburgh, PA). KCl was product of Avantor Performance Materials (Center Valley, PA). Ouabain was purchased from Enzo Life Sciences, Inc. (Farmingdale, NY). Dithiothreitol was a product of Promega Corporation (Madison, WI). MgCl<sub>2</sub> was purchased from EMD Millipore (Billerica, MA). Ascorbic acid was a product of VWR International (West Chester, PA). Sodium orthovanadate was purchased from Alfa Aesar (Ward Hill, MA).

### 2.2 Cell lines and cell culture

The human non-small cell lung carcinoma cell line (NSCLC) H460 was maintained in DMEM based media and its MX resistant cell line, H460/MX20, was maintained in DMEM based media in the presence of 20 nM MX [33]. Wild-type ABCG2-482-R2, mutant ABCG2-482-G2, and mutant ABCG2-482-T7 cells were established as previously described [34]. The HEK293/ABCB1 cell line was generated by transfecting HEK293 cells with vectors that express ABCB1 [19]. Cells were cultured at 37°C in a humidified incubator containing 5% CO<sub>2</sub>. When cells were 60% to 80% confluent, they were harvested and used for in vitro studies.

### 2.3 Cytotoxicity assays

*In vitro*, the cell sensitivity to each antineoplastic drug was determined by a modified MTT assay [12,35]. Briefly, each well of 96 well plates contained approximately 3000 H460 cells or H460/MX20 cells. Cells were collected, re-suspended in media, and seeded evenly in 96-well plates and incubated for 24 h at 37°C. Then, 20 µL of a predetermined, fixed concentration of cabozantinib was added into each well. After 1 h of incubation, 20 µL of the respective antineoplastic drugs were added into each well, serially diluted. After 72 h of incubation, 20 µL of 4mg/ml MTT solution was added to each well. The plates were incubated at 37°C for 4 hours in the presence of the MTT solution. Finally, the MTT-medium was removed and 100 µl DMSO was added to each well to terminate the staining. Absorbance values of the samples were measured at 570 nm using Opsys microplate reader (Dynex Technologies, Chantilly, VA).

### 2.4 Mitoxantrone intracellular accumulation study

H460 and H460/MX20 cells were equally seeded on coverslips in 6-well plates, incubated at 37°C overnight. Cells were washed with phosphate-buffered saline (PBS), and incubated with or without 5 µM cabozantinib for 1 h before incubating with 5 µM MX for 2 h. After the cells were washed with ice-cold PBS, the images were collected using a Nikon TE-2000S fluorescence microscope with an APO 60X oil immersion lens (Nikon). MX fluorescence was excited and collected using the Nikon TRITC HYQ excitation filter combination [36,37].

### 2.5 [<sup>3</sup>H]-MX accumulation and efflux assay

The effect of cabozantinib on the intracellular accumulation and efflux of [<sup>3</sup>H]-MX was determined in ABCG2-overexpressing cells as previous described [38]. Briefly, the H460 cells and H460/MX20 cells were harvested at 80% confluency. Approximately  $5 \times 10^6$  cells were cultured in 37°C in DMEM, supplemented with 10% FBS, with or without cabozantinib (5 or 10 µM) or FTC (10 µM) for 2 h. Subsequently, H460 and H460/MX20 cells were incubated with 0.1 µM [<sup>3</sup>H]-MX medium in the presence or absence of ABCG2 inhibitors for 2 h. Then the cells were washed with cold phosphate-buffered saline (PBS) and collected with 200 µl lysis buffer (pH 7.4, containing 1% Triton X-100 and 0.2% SDS). The sample was placed in scintillation fluid in respective vials. The radioactivity of each sample was measured by a Packard Tri-Carb 1900CA liquid scintillation analyzer (Packard Instrument Company, Inc. Downers Grove, IL). In the efflux study, H460 and H460/MX20 were prepared as described in the accumulation experiment. After rinsing 3 times with PBS, cells were incubated with or without cabozantinib (5 or 10 µM) or FTC (10 µM) at 37°C. The cells were then harvested at various time points (0, 30, 60, 120 min) and radioactivity from the cell lysate was determined using the liquid scintillation counter (Packard Instrument, IL) [39,40].

### 2.6 Western blot analysis

H460, H460/MX20 cell lines were incubated with 5 µM cabozantinib for 0, 24, 48, and 72 h. The cells were harvested and washed 3 times with PBS. The cell extracts were lysed using a lysis buffer (pH 7.4, containing 1% Triton X-100 and 0.2% SDS) for 20 min on ice and the

cells were centrifuged at  $16000 \times g$  for 15 min at  $4^{\circ}\text{C}$ . The cell lysates were run on an SDS-PAGE gel and electrophoretically transferred onto polyvinylidene fluoride (PVDF) membranes. We used a blocking solution containing 5% non-fat milk in TBST buffer [10 mM Tris-base, 10 mM NaCl and 0.1% Tween-20] to incubate the membrane at room temperature for 2 h. Subsequently, the membranes were incubated overnight with a primary monoclonal antibody against ABCG2 (1:400 dilution) or  $\beta$ -actin (1:400 dilution) at  $4^{\circ}\text{C}$  and were further incubated with a horseradish peroxidase (HRP)-conjugated secondary anti-mouse antibody (1:1000 dilution). The reaction was visualized by means of enhanced chemiluminescence detection reagents (Amersham, NJ, USA) following the manufacturer's protocol [41].

## 2.7 Immunofluorescence assays

H460, H460/MX20 cells were seeded in 24-well plates and incubated with or without  $10 \mu\text{M}$  cabozantinib for 72 h at  $37^{\circ}\text{C}$ . Subsequently, PE-conjugated anti-Hu CD338 (ABCG2) (1:200) were used to incubate the cells overnight. Nuclei were counterstained by 2-(4-Amidinophenyl)-6-indolecarbamidine dihydrochloride (DAPI). Images were taken by a Nikon TE2000S microscope [42].

## 2.8 ABCG2 ATPase assay

The vanadate-sensitive ATPase activity of ABCG2 was measured by PREDEASY ATPase Kits with modified protocols. The ABCG2-membranes were thawed and diluted. The membranes ( $20 \mu\text{g}$  protein/reaction) were incubated in ATPase assay buffer at  $37^{\circ}\text{C}$  for 5 min with or without  $400 \mu\text{M}$  vanadate. The membrane vesicles were incubated with different concentrations of cabozantinib, ranging from 0 to  $40 \mu\text{M}$ , at  $37^{\circ}\text{C}$  for 5 min, followed by an addition of  $10 \mu\text{L}$  of 25 mM Mg-ATP solution. The reaction continued to run for another 20 min at  $37^{\circ}\text{C}$ , and then was terminated by an addition of  $100 \mu\text{L}$  5% SDS solution to the reaction mix. The amount of inorganic phosphate (Pi) released was detected and quantified by adding of  $200 \mu\text{L}$  of detection reagent. The reaction mix was then further incubated for 10 min at room temperature. The absorption was detected at 880 nm using a spectrophotometer [39].

## 2.9 Molecular docking analysis with cabozantinib

Cabozantinib structure was built and prepared using our previous molecular modeling protocols [35]. ABCG2 docking grid was generated by selecting significant residues (Asn<sup>387</sup>, Gln<sup>398</sup>, Thr<sup>402</sup>, Arg<sup>482</sup>, Asn<sup>629</sup>, Thr<sup>642</sup> and Tyr<sup>645</sup>) at the centroid of the transmembrane domain as centroid [6,43]. Glide XP docking protocol (Schrödinger, LLC, New York, NY) was followed to dock all prepared 100 cabozantinib conformations into ABCG2. Multiple docking poses were ranked by Glide Emodel value [44] and the top-scoring cabozantinib conformation was used for graphical analysis. All computations were carried out on a 6-core Intel Xeon processor with a Mac OS.

## 2.10 Statistical analysis

All experiments were repeated at least three times and the difference was evaluated by one-way ANOVA.  $P < 0.05$  was considered statistically significant. Statistical analysis was performed using GraphPad Prism version 6.01 for Mac (GraphPad Software, La Jolla, CA).

## 3. Results

### 3.1 The influence of cabozantinib in reversing ABCG2-mediated MDR

*In vitro* cytotoxicity of cabozantinib alone was first determined using the survival rate of H460 cells and H460/MX20 drug-induced and transfected cells via the MTT assay. As shown in Fig 1A and Fig 1B, cabozantinib did not show significant cytotoxicity at 8  $\mu\text{M}$  in H460 and H460/MX20 cells, as well as in HEK293/pcDNA3.1 and in ABCG2-482-R2, ABCG2-482-G2, and ABCG2-482-T7 cell lines. Based on these results, we used 5  $\mu\text{M}$  as the highest concentration to treat the cells. We studied the effect of cabozantinib at concentrations of 2.5 and 5  $\mu\text{M}$  on the H460 and H460/MX20 cells with the antineoplastic drugs MX, topotecan, and SN38 (Fig 1B). As shown in Table 1, at concentrations of 2.5 and 5  $\mu\text{M}$ , cabozantinib can significantly sensitize the ABCG2-overexpressing H460/MX20 cells to the antineoplastic drug MX, topotecan, and SN-38. However, cabozantinib at 5  $\mu\text{M}$  did not change the  $\text{IC}_{50}$  of these substrate drugs in the parental cell line, H460 (Table 1). Similarly, pre-incubation with 2.5 and 5  $\mu\text{M}$  of cabozantinib can also increase the response of antineoplastic drug MX, topotecan, and SN-38 in ABCG2 transfected cell lines ABCG2-482-R2, ABCG2-482-G2, and ABCG2-482-T7 (Table 2). The response of the ABCG2 transfected cell lines to the ABCG2 substrate drugs (MX, topotecan, SN-38) was lower than that of the parental HEK293 cells. The reversal efficacy of cabozantinib on ABCG2 expressing cell lines H460/MX20, ABCG2-482-R2, ABCG2-482-G2, ABCG2-482-T7 was comparable to the well-known ABCG2 inhibitor FTC (5  $\mu\text{M}$ ). Cisplatin served as a negative control antineoplastic drug, as it is not a substrate of ABCG2 (Table 1,2). As shown in Table 1, cabozantinib, at 5  $\mu\text{M}$ , cannot significantly alter the sensitivity of ABCG2-overexpressing cell lines to cisplatin. Moreover, cabozantinib did not significantly alter the sensitivity of HEK293/ABCB1 cells to anticancer drugs (Table 2). Based on the aforementioned results, cabozantinib can effectively sensitize ABCG2 substrate resistant cancer cells in a mechanism specific to ABCG2 inhibition (Table 3).

### 3.2 The influence of cabozantinib in increasing accumulation of [ $^3\text{H}$ ]-MX in ABCG2-overexpressing cell

In order to reveal the mechanism of cabozantinib in reversing ABCG2-mediated MDR, we measured the effect of cabozantinib in increasing intracellular concentrations of [ $^3\text{H}$ ]-MX in the parental H460 cells, as well as ABCG2 overexpressing H460/MX20 cells. We also examined the effect of cabozantinib on the intracellular accumulation of [ $^3\text{H}$ ]-MX of transfected ABCG2-482-R2, ABCG2-482-G2, and ABCG2-482-T7 cells. As shown in Fig 2A and 2C, intracellular accumulation of [ $^3\text{H}$ ]-MX was significantly higher in the H460 control group, compared to that of the ABCG2 overexpressing cell lines H460/MX20 (Fig 2A), ABCG2-482-R2, ABCG2-482-G2, and ABCG2-482-T7 (Fig 2C). However, cabozantinib (at 5  $\mu\text{M}$  and 10  $\mu\text{M}$ ) significantly reversed the accumulation of [ $^3\text{H}$ ]-MX to a level that is comparable to that of the H460 or HEK293 parental cells. The efficacy of

cabozantinib on increasing intracellular accumulation of [<sup>3</sup>H]-MX in resistant cell line is comparable to that of FTC. These results suggest that cabozantinib can potentiate the cytotoxicity of MX by increasing its intracellular accumulation in the otherwise resistant cells.

### 3.3 The effect of cabozantinib on the efflux of [<sup>3</sup>H]-MX in the ABCG2-overexpressing cells

We used efflux assays to determine whether cabozantinib can significantly decrease the efflux function in the parental cell lines H460 and HEK293, as well as ABCG2-overexpressing cell lines H460/MX20, ABCG2-482-R2, ABCG2-482-G2, and ABCG2-482-T7. As shown in Fig 2B and Fig 2D, the efflux of [<sup>3</sup>H]-MX from ABCG2 overexpressing cell lines H460/MX20 (Fig 2B), ABCG2-482-R2, ABCG2-482-G2, and ABCG2-482-T7 (Fig 2D) was significantly higher than that of H460 and HEK293 cell lines. The incubation of cabozantinib (10 μM) with ABCG2 overexpressing cell line can significantly increase the intracellular concentration of [<sup>3</sup>H]-MX over increasing periods of time (0, 30, 60, 120 min). Furthermore, results show cabozantinib can potentiate the cytotoxicity of ABCG2-overexpressing cell line by decreasing the efflux function of ABCG2 protein.

### 3.4 The influence of cabozantinib in increasing intracellular accumulation of MX fluorescence in ABCG2-overexpressing cell line

In order to elucidate the mechanism by which cabozantinib increases the response of ABCG2-overexpressing cells to the respective substrate drugs, we also examined the intracellular accumulation of MX fluorescence. As Shown in Fig 3, incubation of H460 cells with or without 5 μM of cabozantinib did not alter intracellular accumulation of MX. However, in the H460/MX20 cell line, 5 μM cabozantinib could significantly increase the fluorescence of MX inside the cells.

### 3.5 The effect of cabozantinib on the expression of the ABCG2 protein

In order to further understand the mechanism by which cabozantinib sensitizes these ABCG2 overexpressing cells to the anticancer drugs, Western blotting assays were performed to examine the effect of cabozantinib on the expression level of the ABCG2 protein. Fig 4 demonstrates that incubating H460/MX20 at various time points for up to 72 hours did not alter the expression of the ABCG2 protein. Thus it is unlikely that cabozantinib's reversal effect is due to a downregulation of the ABCG2 protein expression.

### 3.6 The effect of cabozantinib on the subcellular localization of ABCG2 transporter

In order to determine whether cabozantinib can alter the subcellular localization of the ABCG2 transporter, we performed an immunofluorescence assay, comparing the parental and ABCG2 overexpressing cells. We incubated H460/MX20 cells with 5 μM cabozantinib for 0 h and 72 h. As shown in Fig 5, the subcellular distribution of ABCG2 incubated with cabozantinib for 72 hours did not change compared to the cells incubated in the absence of cabozantinib. Therefore, our results indicate that cabozantinib does not alter the cellular localization of the ABCG2 transporter.

### 3.7 The effect of cabozantinib on the ABCG2 ATP hydrolysis

The ABCG2 transporter utilizes energy derived from the hydrolysis of ATP to efflux its substrates across the membrane against a concentration gradient; thus ATP consumption reflects its ATPase activity [42]. To assess the effect of cabozantinib on the ATPase activity of ABCG2, we measured ABCG2-mediated ATP hydrolysis in the presence of cabozantinib at various concentrations from 0 to 40  $\mu\text{M}$ . Similar to other TKIs, cabozantinib stimulated the ATPase activity of ABCG2 in a concentration-dependent manner, with a maximal stimulation of 2.70-fold of the basal activity (Fig. 6A and Fig 6B). The concentration of cabozantinib required to obtain 50% stimulation is 0.734  $\mu\text{M}$ . The results indicate that cabozantinib interacts at the drug-substrate-binding site and affects the ATPase activity of the ABCG2 transporter.

### 3.8 Molecular docking analysis of cabozantinib with human ABCG2 homology model

Since previous results indicated that cabozantinib may have direct interaction with ABCG2 at transmembrane domain as a potential substrate, we performed a molecular docking simulation of cabozantinib on the ABCG2 homology model. Cabozantinib exhibited a Glide XP score of  $-8.517$ . As shown in Figure 7, the majority of cabozantinib molecule was stabilized into a cavity formed by hydrophobic residues Tyr<sup>464</sup>, Phe<sup>489</sup>, Phe<sup>507</sup>, Val<sup>508</sup>, Phe<sup>511</sup>, Met<sup>515</sup>, Ile<sup>573</sup>, Pro<sup>574</sup>, Tyr<sup>576</sup>, Ala<sup>580</sup>, Leu<sup>581</sup>, Leu<sup>626</sup>, Trp<sup>627</sup>, Ala<sup>632</sup> and Leu<sup>633</sup>. A  $\pi$ - $\pi$  interaction was formed between the ligand phenyl ring and imidazole ring of His<sup>630</sup>. No hydrogen bonding interactions were predicted in the docked pose of cabozantinib.

## 4. Discussion

Our study is the first to demonstrate that cabozantinib can significantly sensitize cell lines with ABCG2-induced drug resistance to the substrate anticancer drugs MX, topotecan, and SN-38. In clinical trials, patients received cabozantinib orally from 60 mg to 140 mg to treat medullary thyroid carcinoma [32]. The pharmacokinetics study in which patients are given 175 mg cabozantinib daily with samples collected on day 19 showed that the  $C_{\text{max}}$  in the blood is 2310 ng/mL, and SD value is around 884 ng/mL (approximately 2.8 to 6.4  $\mu\text{M}$ ) [45]. In our study, the highest concentration of cabozantinib used as a reversal agent was 5  $\mu\text{M}$ , which is within the range of clinical concentration of cabozantinib. Even though there is a study demonstrating that VEGFR is expressed in H460 cells, the dose of cabozantinib we used was not enough to inhibit the proliferation of the cells (Fig 2). Cabozantinib's sensitizing effect on MDR cells may benefit drug resistant patients with a potential novel combinational chemotherapy.

Our study clearly revealed that cabozantinib functioned as a reversing agent that specifically targets the ABCG2 protein. The maximum reversal concentration of cabozantinib is 5  $\mu\text{M}$ , which is close to the blood concentration of cabozantinib in patients after repeated treatments. In the present study, cabozantinib (at 2.5 and 5  $\mu\text{M}$ ) significantly reduced the  $\text{IC}_{50}$  value of MX, SN-38, and topotecan. In order to exclude other factors that cause MDR, we also used transfected cell lines HEK293/pcDNA3.1, ABCG2-482-R2, ABCG2-482-T7, and ABCG2-482-G2 to conduct our study. Our MTT results showed that 5  $\mu\text{M}$  of cabozantinib can significantly increase the cytotoxic effects of ABCG2 substrates in



transfected cells. These results indicated that cabozantinib's reversal activity was not only limited to wild-type ABCG2 overexpressing cell lines, but also in mutant ABCG2 overexpressing cell lines.

We also examined the possibility of cabozantinib's activity in reversing ABCB1-mediated MDR by conducting MTT assays. Although this result, contradicts to that of Xiang's previous study [46], the discrepancy between our study and the previous study conducted by Xiang and colleagues may be due to utilization of different cell lines, since they used HepG2/adr and HepG2 cells in their study.

Accumulation study results showed that cabozantinib significantly increased the intracellular accumulation of [<sup>3</sup>H]-MX in ABCG2 overexpressing cells. The increasing intracellular accumulation of [<sup>3</sup>H]-MX was also found in ABCG2-482-R2, ABCG2-482-T7, and ABCG2-482-G2 transfected cells. These results indicated that cabozantinib can increase intracellular accumulation of [<sup>3</sup>H]-MX in both wild-type and mutant ABCG2-overexpressing cells.

The reversal mechanisms mediated by ABC transporter modulators could be due to downregulation of the protein expression of the ABC transporter, or by inhibiting the efflux function. In order to further investigate the mechanism of cabozantinib in reversing MDR, we performed additional experiments and found that cabozantinib significantly inhibits the efflux function of ABCG2. Moreover, Western blotting results demonstrated that cabozantinib treatment does not significantly alter the ABCG2 protein expression. Immunofluorescence also indicated that cabozantinib did not significantly affect the translocation of ABCG2 protein compared to the control group. Furthermore, cabozantinib stimulated the ATPase activity of ABCG2 in a concentration-dependent manner, with a maximal stimulation of 2.70-fold of the basal activity. Taken together, our study suggests that cabozantinib significantly sensitizes ABCG2-overexpressing cells to substrate antineoplastic drugs by inhibiting the efflux function of the transporter. The molecular docking simulations predicted that cabozantinib was stabilized into the transmembrane domain of ABCG2 via hydrophobic interactions. These results suggest that cabozantinib might inhibit ABCG2 competitively as an ABCG2 substrate.

In conclusion, our study demonstrates that cabozantinib significantly increases the cytotoxicity of antineoplastic drugs including MX, topotecan, and SN38 in cells that overexpress ABCG2 transporter by blocking the transporter's efflux function. This study suggests that the combined use of cabozantinib with a conventional antineoplastic agent is a promising strategy to overcome ABCG2-mediated MDR in various types of cancer.

## Supplementary Material

Refer to Web version on PubMed Central for supplementary material.

## Acknowledgments

Funding: this work was supported by funds from NIH (No. 1R15CA143701) and St. John's University research Seed Grant (No. 579-1110-7002) to Z.S.Chen.

We thank Dr. Mark F. Rosenberg (University of Manchester, Manchester, UK) and Dr. Zsolt Bikádi (Virtua Drug Ltd., Budapest, Hungary) for providing coordinates of ABCG2 homology model, Drs. Susan E. Bates and Robert W. Robey (NIH, Bethesda, MD) for FTC, H460, H460/MX20. HEK293/pcDNA 3.1 and the ABCG2 transfected cell lines. We thank ChemieTek, (Indianapolis, IN) for providing us with free sample of cabozantinib. We thank Dr. Yangmin Chen (ICON plc, North Wales, PA) for editing the English of the article.

## Abbreviations

<b>MDR</b>	multidrug resistant
<b>ABC transporter</b>	ATP binding cassette transporter
<b>ABCG2</b>	TP-binding cassette subfamily G member 2

## References

- Ejendal KF, Hrycyna CA. Multidrug Resistance and Cancer: The Role of the Human ABC Transporter ABCG2. *Curr Protein Pept Sci.* 2002; 3:503–511. DOI: 10.2174/1389203023380521 [PubMed: 12369998]
- Zhang YK, Wang YJ, Gupta P, Chen ZS. Multidrug Resistance Proteins (MRPs) and Cancer Therapy. *Aaps J.* 2015; 17:802–812. DOI: 10.1208/s12248-015-9757-1 [PubMed: 25840885]
- Sharom FJ. ABC multidrug transporters: structure, function and role in chemoresistance. 2007; 9:105–127. <http://Dx.Doi.org/10.2217/14622416.9.1.105>. DOI: 10.2217/14622416.9.1.105
- Mao Q, Unadkat JD. Role of the breast cancer resistance protein (ABCG2) in drug transport. *Aaps J.* 2005; 7:E118–33. DOI: 10.1208/aapsj070112 [PubMed: 16146333]
- Doyle LA, Yang W, Abruzzo LV, Krogmann T, Gao Y, Rishi AK, et al. A multidrug resistance transporter from human MCF-7 breast cancer cells. *Proc Natl Acad Sci USA.* 1998; 95:15665–15670. DOI: 10.1073/pnas.95.26.15665 [PubMed: 9861027]
- Ni Z, Bikadi Z, Rosenberg MF, Mao Q. Structure and function of the human breast cancer resistance protein (BCRP/ABCG2). *Curr Drug Metab.* 2010; 11:603–617. [PubMed: 20812902]
- Miyake K, Mickley L, Litman T, Zhan Z, Robey R, Cristensen B, et al. Molecular cloning of cDNAs which are highly overexpressed in mitoxantrone-resistant cells: demonstration of homology to ABC transport genes. *Cancer Res.* 1999; 59:8–13. [PubMed: 9892175]
- Cole SP, Chanda ER, Dicke FP, Gerlach JH, Mirski SE. Non-P-glycoprotein-mediated multidrug resistance in a small cell lung cancer cell line: evidence for decreased susceptibility to drug-induced DNA damage and reduced levels of topoisomerase II. *Cancer Res.* 1991; 51:3345–3352. [PubMed: 1675932]
- Ross DD, Yang W, Abruzzo LV, Dalton WS, Schneider E, Lage H, et al. Atypical multidrug resistance: breast cancer resistance protein messenger RNA expression in mitoxantrone-selected cell lines. *JNCI J Natl Cancer Inst.* 1999; 91:429–433. DOI: 10.1093/jnci/91.5.429 [PubMed: 10070941]
- Maliepaard M, van Gastelen MA, de Jong LA, Pluim D, van Waardenburg RC, Ruevekamp-Helmers MC, et al. Overexpression of the BCRP/MXR/ABCP gene in a topotecan-selected ovarian tumor cell line. *Cancer Res.* 1999; 59:4559–4563. [PubMed: 10493507]
- Allen JD, Brinkhuis RF, Wijnholds J, Schinkel AH. The Mouse *Bcrp1/Mxr/Abcp* Gene. *Cancer Res.* 1999; 59:4237–4241. DOI: 10.1016/0092-8674(86)90595-7 [PubMed: 10485464]
- Anreddy N, Patel A, Zhang YK, Wang YJ, Shukla S, Kathawala RJ, et al. A-803467, a tetrodotoxin-resistant sodium channel blocker, modulates ABCG2-mediated MDR in vitro and in vivo. *Oncotarget.* 2015; 6:39276–39291. DOI: 10.18632/oncotarget.5747 [PubMed: 26515463]
- Huber S, Wege AK, Bernhardt G, Buschauer A, Brockhoff G. Topotecan-induced ABCG2 expression in MCF-7 cells is associated with decreased CD24 and EpCAM expression and a loss of tumorigenicity. *Cytometry A.* 2015; 87:707–716. DOI: 10.1002/cyto.a.22675 [PubMed: 25892097]
- Hasanabady MH, Kalalinia F. ABCG2 inhibition as a therapeutic approach for overcoming multidrug resistance in cancer. *J Biosci.* 2016; 41:313–324. [PubMed: 27240991]

15. Komeili-Movahhed T, Fouladdel S, Barzegar E, Atashpour S, Hossein Ghahremani M, Nasser Ostad S, et al. PI3K/Akt inhibition and down-regulation of BCRP re-sensitize MCF7 breast cancer cell line to mitoxantrone chemotherapy. *Iran J Basic Med Sci.* 2015; 18:472–477. [PubMed: 26124933]
16. Wang XK, To KKW, Huang LY, Xu JH, Yang K, Wang F, et al. Afatinib circumvents multidrug resistance via dually inhibiting ATP binding cassette subfamily G member 2 in vitro and in vivo. *Oncotarget.* 2014; 5:11971–11985. DOI: 10.18632/oncotarget.2647 [PubMed: 25436978]
17. Zhang YK, Zhang GN, Wang YJ, Patel BA, Talele TT, Yang DH, et al. Bafetinib (INNO-406) reverses multidrug resistance by inhibiting the efflux function of ABCB1 and ABCG2 transporters. *Sci Rep.* 2016; 6:25694.doi: 10.1038/srep25694 [PubMed: 27157787]
18. Yang D, Kathawala RJ, Chufan EE, Patel A, Ambudkar SV, Chen ZS, et al. Tivozanib reverses multidrug resistance mediated by ABCB1 (P-glycoprotein) and ABCG2 (BCRP). *Future Oncology.* 2014; 10:1827–1841. DOI: 10.2217/fon.13.253 [PubMed: 24295377]
19. Guo HQ, Zhang GN, Wang YJ, Zhang YK, Sodani K, Talele TT, et al.  $\beta$ -Elemene, a compound derived from *Rhizoma zedoariae*, reverses multidrug resistance mediated by the ABCB1 transporter. *Oncol Rep.* 2014; 31:858–866. DOI: 10.3892/or.2013.2870 [PubMed: 24284783]
20. de Bruin M, Miyake K, Litman T, Robey R, Bates SE. Reversal of resistance by GF120918 in cell lines expressing the ABC half-transporter, MXR. *Cancer Lett.* 1999; 146:117–126. DOI: 10.1016/S0304-3835(99)00182-2 [PubMed: 10656616]
21. Tiwari AK, Sodani K, Wang S-R, Kuang Y-H, Ashby CR Jr, Chen X, et al. Nilotinib (AMN107, Tasisign<sup>®</sup>) reverses multidrug resistance by inhibiting the activity of the ABCB1/Pgp and ABCG2/BCRP/MXR transporters. *Biochem Pharmacol.* 2009; 78:153–161. DOI: 10.1016/j.bcp.2009.04.002 [PubMed: 19427995]
22. Tiwari AK, Sodani K, Dai CL, Abuznait AH, Singh S, Xiao ZJ, et al. Nilotinib potentiates anticancer drug sensitivity in murine ABCB1-, ABCG2-, and ABCC10-multidrug resistance xenograft models. *Cancer Lett.* 2013; 328:307–317. DOI: 10.1016/j.canlet.2012.10.001 [PubMed: 23063650]
23. Kurzrock R, Sherman SI, Ball DW, Forastiere AA, Cohen RB, Mehra R, et al. Activity of XL184 (Cabozantinib), an oral tyrosine kinase inhibitor, in patients with medullary thyroid cancer. *J Clin Oncol.* 2011; 29:2660–2666. DOI: 10.1200/JCO.2010.32.4145 [PubMed: 21606412]
24. Yakes FM, Chen J, Tan J, Yamaguchi K, Shi Y, Yu P, et al. Cabozantinib (XL184), a Novel MET and VEGFR2 Inhibitor, Simultaneously Suppresses Metastasis, Angiogenesis, and Tumor Growth. *Mol Cancer Ther.* 2011; 10:2298–2308. DOI: 10.1158/1535-7163.MCT-11-0264 [PubMed: 21926191]
25. Smith DC, Smith MR, Sweeney C, Elfiky AA, Logothetis C, Corn PG, et al. Cabozantinib in patients with advanced prostate cancer: results of a phase II randomized discontinuation trial. *J Clin Oncol.* 2013; 31:412–419. DOI: 10.1200/JCO.2012.45.0494 [PubMed: 23169517]
26. Vaishampayan U. Cabozantinib as a novel therapy for renal cell carcinoma. *Curr Oncol Rep.* 2013; 15:76–82. DOI: 10.1007/s11912-012-0289-x [PubMed: 23292795]
27. Smith MR, Sweeney CJ, Corn PG, Rathkopf DE, Smith DC, Hussain M, et al. Cabozantinib in chemotherapy-pretreated metastatic castration-resistant prostate cancer: results of a phase II nonrandomized expansion study. *J Clin Oncol.* 2014; 32:3391–3399. DOI: 10.1200/JCO.2013.54.5954 [PubMed: 25225437]
28. Yavuz S, Apolo AB, Kummur S, del Rivero J, Madan RA, Shawker T, et al. Cabozantinib-induced thyroid dysfunction: a review of two ongoing trials for metastatic bladder cancer and sarcoma. *Thyroid.* 2014; 24:1223–1231. DOI: 10.1089/thy.2013.0621 [PubMed: 24724719]
29. Apolo, AB., Parnes, HL., RA, Madan, HL., Gulley, JL., Wright, JJ. A phase II study of cabozantinib in patients (pts) with relapsed or refractory metastatic urothelial carcinoma (mUC). *ASCO Annual Meeting ...*; 2014;
30. Buckanovich, RJ., Berger, R., Sella, A., Sikic, BI., Shen, X. Activity of cabozantinib (XL184) in advanced ovarian cancer patients (pts): Results from a phase II randomized discontinuation trial (RDT). *ASCO Annual Meeting ...*; 2011;

31. Cohn, AL., Kelley, RK., Yang, TS., Su, WC., Verslype, C. Activity of cabozantinib (XL184) in hepatocellular carcinoma patients (pts): Results from a phase II randomized discontinuation trial (RDT). ASCO Annual Meeting ...; 2012;
32. Drilon A, Rekhtman N, Arcila M, Wang L, Ni A, Albano M, et al. Cabozantinib in patients with advanced RET-rearranged non-small-cell lung cancer: an open-label, single-centre, phase 2, single-arm trial. *The Lancet Oncology*. 2016; doi: 10.1016/S1470-2045(16)30562-9
33. Henrich CJ, Bokesch HR, Dean M, Bates SE, Robey RW, Goncharova EI, et al. A High-Throughput Cell-Based Assay for Inhibitors of ABCG2 Activity. *J Biomol Screen*. 2006; 11:176–183. DOI: 10.1177/1087057105284576 [PubMed: 16490770]
34. Zhang H, Kathawala RJ, Wang YJ, Zhang YK, Patel A, Shukla S, et al. Linsitinib (OSI-906) antagonizes ATP-binding cassette subfamily G member 2 and subfamily C member 10-mediated drug resistance. *Int J Biochem Cell Biol*. 2014; 51:111–119. DOI: 10.1016/j.biocel.2014.03.026 [PubMed: 24726739]
35. Marion MB. A rapid and sensitive method for the quantitation of microgram quantities of protein utilizing the principle of protein-dye binding. *Analytical biochemistry*. 1976
36. Patel A, Tiwari AK, Chufan EE, Sodani K, Anreddy N, Singh S, et al. PD173074, a selective FGFR inhibitor, reverses ABCB1-mediated drug resistance in cancer cells. *Cancer Chemother Pharmacol*. 2013; 72:189–199. DOI: 10.1007/s00280-013-2184-z [PubMed: 23673445]
37. Zhang H, Patel A, Ma SL, Li XJ, Zhang YK, Yang PQ, et al. In vitro, in vivo and ex vivo characterization of ibrutinib: a potent inhibitor of the efflux function of the transporter MRP1. *Br J Pharmacol*. 2014; 171:5845–5857. DOI: 10.1111/bph.12889 [PubMed: 25164592]
38. Zhang Y-K, Zhang H, Zhang G-N, Wang Y-J, Kathawala RJ, Si R, et al. Semi-synthetic ocotillol analogues as selective ABCB1-mediated drug resistance reversal agents. *Oncotarget*. 2015; 6:24277–24290. [PubMed: 26296969]
39. Wang D-S, Patel A, Shukla S, Zhang Y-K, Wang Y-J, Kathawala RJ, et al. Icotinib antagonizes ABCG2-mediated multidrug resistance, but not the pemetrexed resistance mediated by thymidylate synthase and ABCG2. *Oncotarget*. 2014; 5:4529–4542. [PubMed: 24980828]
40. Zhou WJ, Zhang X, Cheng C, Wang F, Wang XK, Liang YJ, et al. Crizotinib (PF-02341066) reverses multidrug resistance in cancer cells by inhibiting the function of P-glycoprotein. *Br J Pharmacol*. 2012; 166:1669–1683. DOI: 10.1111/j.1476-5381.2012.01849.x [PubMed: 22233293]
41. WYJ, HY, ANZ, GNZ, YKXM, et al. Tea nanoparticle, a safe and biocompatible nanocarrier, greatly potentiates the anticancer activity of doxorubicin. *Oncotarget*. 2016; 7:5877–5891. DOI: 10.18632/oncotarget.6711 [PubMed: 26716507]
42. Wang DS, Patel A, Sim HM, Zhang YK, Wang YJ, Kathawala RJ, et al. ARRY-334543 reverses multidrug resistance by antagonizing the activity of ATP-binding cassette subfamily G member 2. *J Cell Biochem*. 2014; 115:1381–1391. DOI: 10.1002/jcb.24787 [PubMed: 24939447]
43. Jani M, Ambrus C, Magnan R, Jakab KT, Beery E, Zolnerciks JK, et al. Structure and function of BCRP, a broad specificity transporter of xenobiotics and endobiotics. *Arch Toxicol*. 2014; 88:1205–1248. DOI: 10.1007/s00204-014-1224-8 [PubMed: 24777822]
44. Friesner, Richard A., Murphy, Robert B., Repasky, Matthew P., Frye, Leah L., Greenwood, Jeremy R., Halgren, Thomas A., et al. Extra Precision Glide: Docking and Scoring Incorporating a Model of Hydrophobic Enclosure for Protein Ligand Complexes. *J Med Chem*. 2006; 49:6177–6196. DOI: 10.1021/jm051256o [PubMed: 17034125]
45. Kurzrock R, Sherman SI, Ball DW, Forastiere AA, Cohen RB, Mehra R, et al. Activity of XL184 (Cabozantinib), an Oral Tyrosine Kinase Inhibitor, in Patients With Medullary Thyroid Cancer. *Journal of Clinical Oncology*. 2016; doi: 10.1200/JCO.2011.36.29.issue-19;subPage:string:Abstract;website:website:asco-site;wgroup:string:Publication
46. Xiang QF, Zhang DM, Wang JN, Zhang HW, Zheng ZY, Yu DC, et al. Cabozantinib reverses multidrug resistance of human hepatoma HepG2/adr cells by modulating the function of P glycoprotein. *Liver International*. 2015; 35:1010–1023. DOI: 10.1111/liv.12524 [PubMed: 24621440]

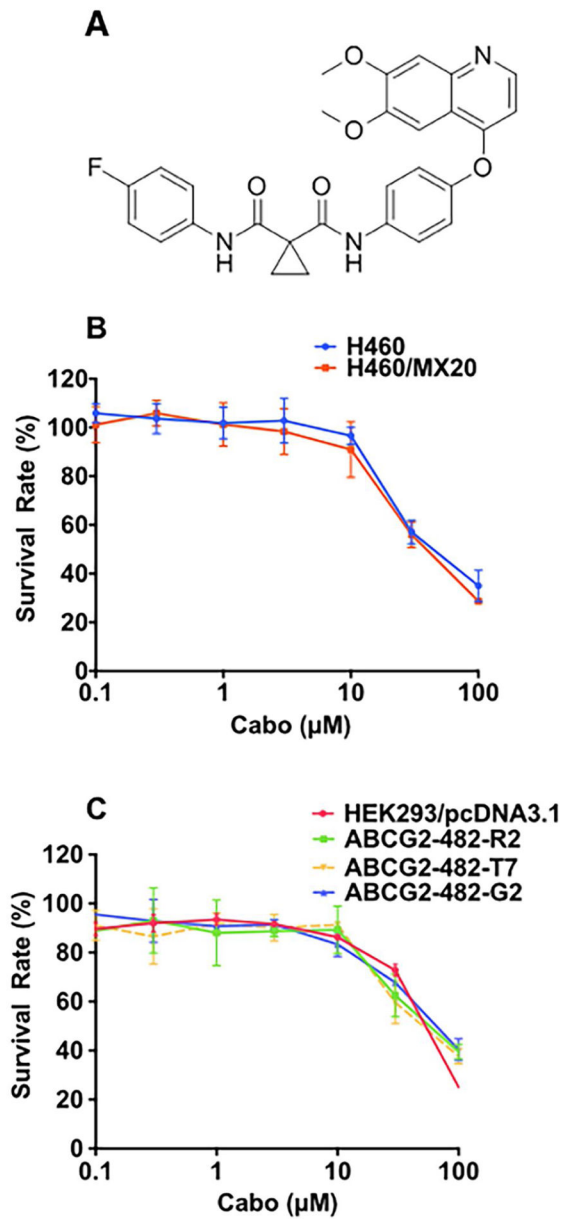


**Fig. 1. Cytotoxicity of cabozantinib in parental cell lines and drug resistant cell lines**  
 (A) Structure of cabozantinib. (B) Cytotoxicity of cabozantinib in H460 and H460/MX20 cells. (C) Cytotoxicity of cabozantinib in HEK293/pcDNA3.1, ABCG2-482-R2, ABCG2-482-G2, ABCG2-482-T7 cells.

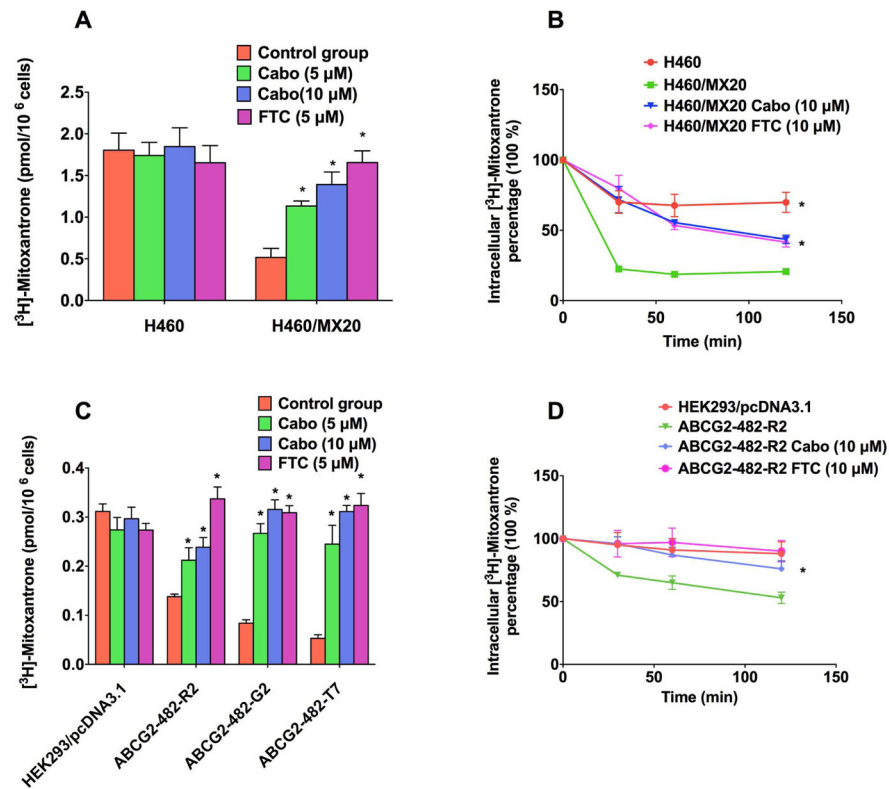


**Fig. 2. Intracellular accumulation of [ $^3$ H]-MX**

(A) The effect of cabozantinib on the cellular accumulation of [ $^3$ H]-MX in H460, H460/MX20 cells. (B). The effect of cabozantinib on the efflux activity of ABCG2 after 30,60, and 120 min of incubation in H460 and H460/MX20 cell lines.

(C). The effect of cabozantinib on cellular accumulation of [ $^3$ H]-MX in HEK293/pcDNA3.1 and ABCG2-293-R2 cells. (D). The effect of cabozantinib on the efflux activity of ABCG2 after 30,60, and 120 min of incubation in HEK293/pcDNA3.1 and ABCG2-293-R2 cell lines.

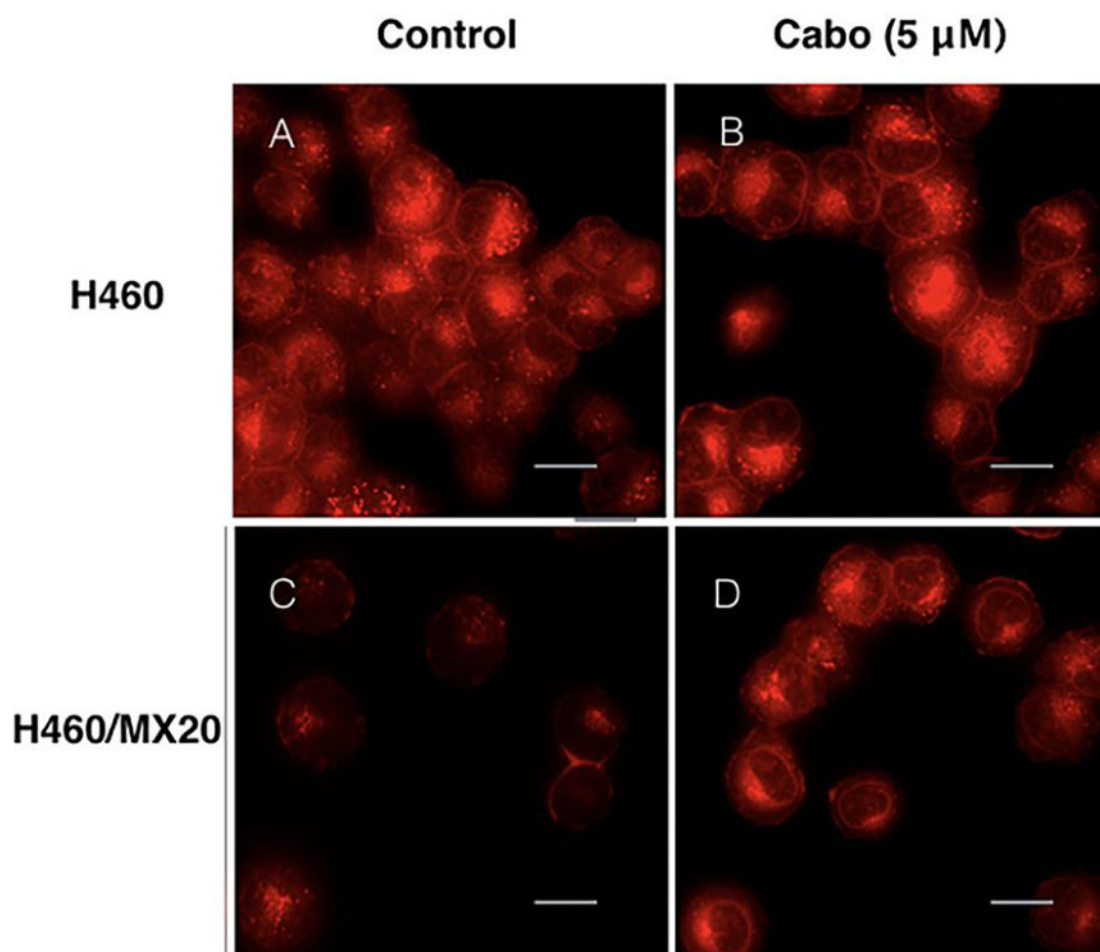


**Fig. 3. Cellular accumulation of MX fluorescence in H460 and H460/MX20**  
MX accumulation fluorescence in H460 and H460/MX20 cell line. H460 and H460/MX20 cells were pretreated or non-pretreated with cabozantinib at 5 μM. Scale bar, 20 μm.

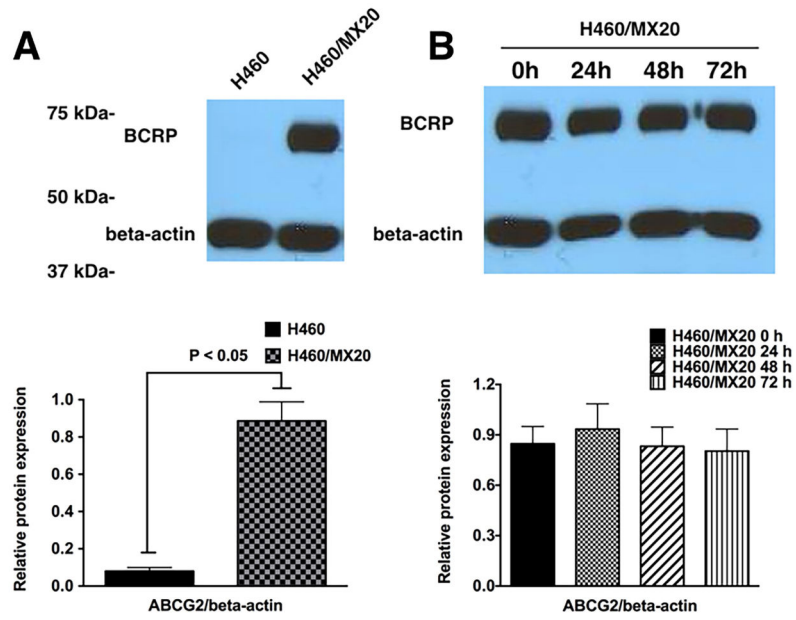


**Fig. 4. The effect of cabozantinib on the expression of ABCG2**  
 (A). Expression of ABCG2 protein in H460 and H460/MX20 cell lines. (B). Analysis of ABCG2 expression in ABCG2-overexpressing H460/MX20 cells in the presence or absence of cabozantinib 5  $\mu$ M for 0, 24, 48 and 72 h.



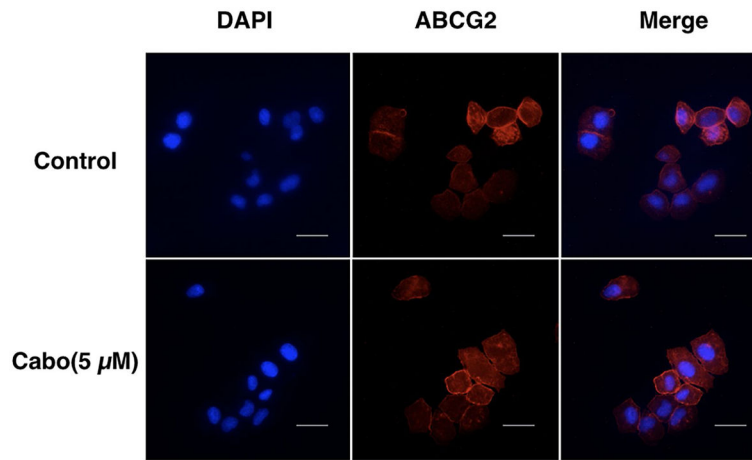


**Fig. 5. Cellular localization of ABCG2 before and after treatment with cabozantinib**  
The localization of ABCG2 after treatment with cabozantinib at 5  $\mu\text{M}$  on H460 parental and H460/MX20 cells overexpressing ABCG2. Scale bar, 20  $\mu\text{m}$  for 72 h.

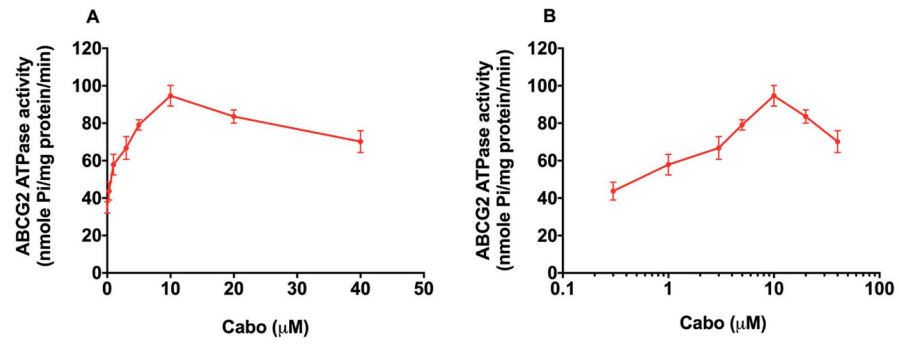


**Fig. 6. Effect of cabozantinib on ABCG2 ATPase activity with increased concentration of cabozantinib (0–40  $\mu\text{M}$ )**

Concentration of cabozantinib was plotted at (A) linear or (B) log scale.

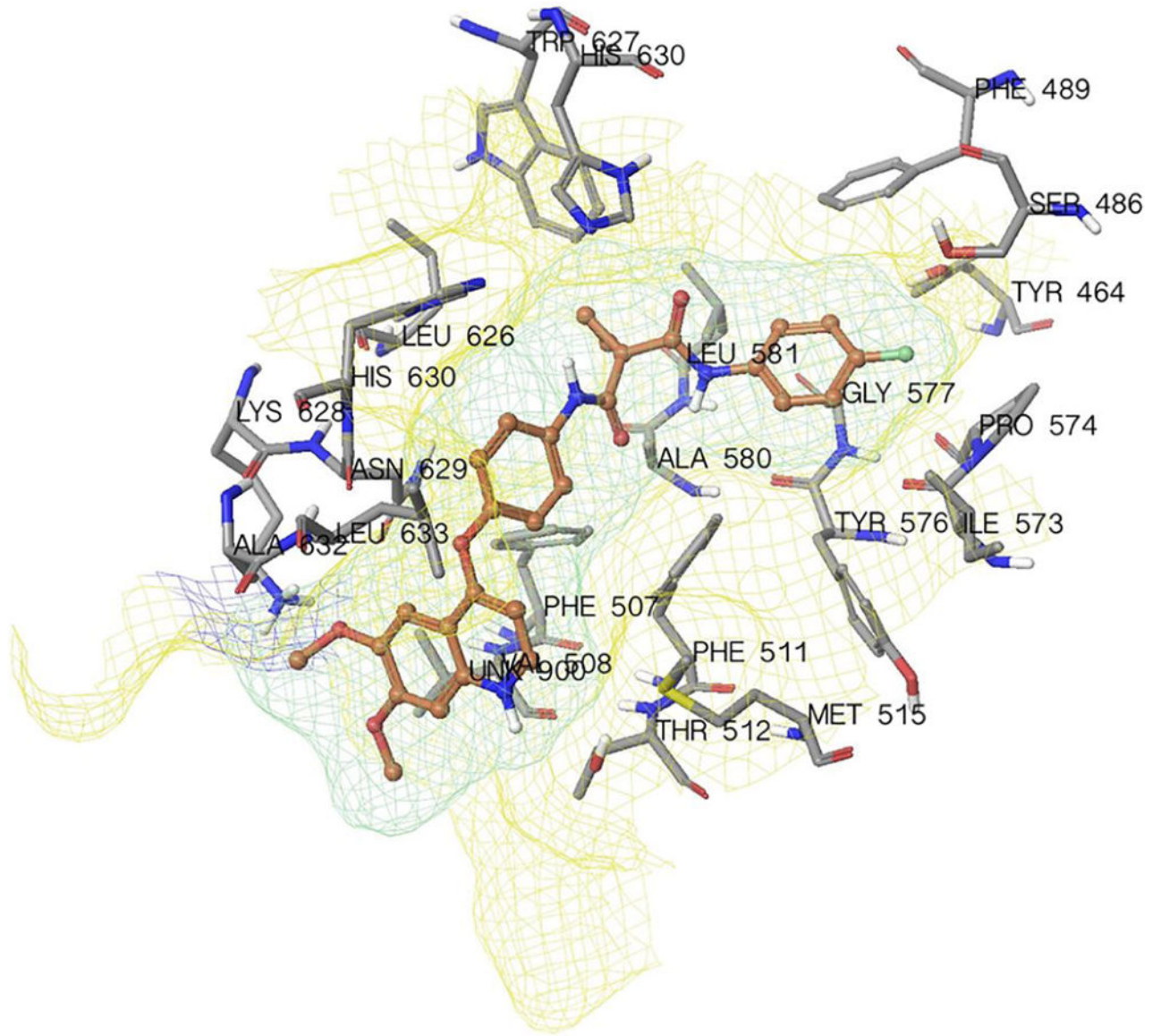


**Fig. 7.**  
Binding geometry of cabozantinib into the ABCG2 binding pocket by the Glide docking algorithms.

**Table 1**

Cabozantinib reverses ABCG2-mediated drug resistance in drug selected resistant cells

Treatment	IC <sub>50</sub> ± SD <sup>a</sup> (μM) (Resistant fold) <sup>b</sup>	
	H460	H460/MX20
<b>Mitoxantrone</b>	0.021 ± 0.005(1.0) <sup>b</sup>	1.533 ± 0.245 (73.1)
+ Cabo 2.5 μM	0.022 ± 0.007(1.0)	0.175 ± 0.021(8.3) *
+ Cabo 5 μM	0.021 ± 0.004(1.0)	0.083 ± 0.032(3.9) *
+ FTC 5 μM	0.022 ± 0.003(1.0)	0.027 ± 0.012(1.3) *
<b>SN-38</b>	0.032 ± 0.002 (1.0)	2.273 ± 0.165(71.0)
+ Cabo 2.5 μM	0.029 ± 0.005(0.9)	0.342 ± 0.031(10.7) *
+ Cabo 5 μM	0.027 ± 0.003(0.8)	0.075 ± 0.006(2.3) *
+ FTC 5 μM	0.029 ± 0.008(0.9)	0.034 ± 0.003(1.0) *
<b>Topotecan</b>	0.077 ± 0.013(1.0)	2.618 ± 0.167(43.23)
+ Cabo 2.5 μM	0.076 ± 0.008(1.0)	0.531 ± 0.017(3.17) *
+ Cabo 5 μM	0.071 ± 0.005(0.9)	0.195 ± 0.014(2.5) *
+ FTC 5 μM	0.070 ± 0.004(0.9)	0.080 ± 0.009(1.03) *
<b>Cisplatin</b>	2.077 ± 0.142(1.0)	2.043 ± 0.293(1.0)
+ Cabo 2.5 μM	1.973 ± 0.178(0.9)	1.973 ± 0.193(1.0)
+ Cabo 5 μM	2.104 ± 0.138(1.0)	2.312 ± 0.132(1.1)
+ FTC 5 μM	2.014 ± 0.291(1.0)	1.991 ± 0.189(1.0)

Cell survival was determined by MTT assay as described in Material and Methods.

<sup>a</sup>IC<sub>50</sub> values are represented as the mean ± standard deviation (SD).

<sup>b</sup>Resistance fold was calculated by the IC<sub>50</sub> values for different substrates, and cisplatin of H460 cell lines with cabozantinib or fumitremogin C (FTC), or the resistant cell line H460/MX20 in the presence or absence of cabozantinib or FTC, divided by the IC<sub>50</sub> values for different substrates, and cisplatin of H460 without the reversing agents.

\* *P* < 0.05, versus the control group.

**Table 2**

The reversal efficacy of cabozantinib in ABCG2-mediated drug resistance in ABCG2-transfected cell lines

Treatments	IC <sub>50</sub> ± SD <sup>a</sup> (μM) (Resistant fold) <sup>b</sup>			
	HEK293/pcDNA3.1	ABCG2-482-R2	ABCG2-482-G2	ABCG2-482-T7
<b>Mitoxantrone</b>	0.032 ± 0.002(1.0) <sup>b</sup>	0.374 ± 0.032(10.8)	0.713 ± 0.067(22.3)	0.273 ± 0.036(8.5)
+ Cabo 2.5 μM	0.031 ± 0.004(1.0)	0.076 ± 0.013(2.3) *	0.115 ± 0.016(3.6) *	0.108 ± 0.011(3.4) *
+ Cabo 5 μM	0.029 ± 0.003(0.9)	0.027 ± 0.003(0.8) *	0.042 ± 0.014(1.3) *	0.034 ± 0.009(1.1) *
+ FTC 5 μM	0.030 ± 0.002(0.9)	0.035 ± 0.007(1.1) *	0.037 ± 0.005(1.2) *	0.030 ± 0.004(0.9) *
<b>SN-38</b>	0.019 ± 0.006(1.0)	0.198 ± 0.022(10.4)	0.214 ± 0.012 (11.3)	0.378 ± 0.024(19.7)
+ Cabo 2.5 μM	0.018 ± 0.007(0.9)	0.097 ± 0.010(5.1) *	0.118 ± 0.013(6.2) *	0.081 ± 0.019(4.3) *
+ Cabo 5 μM	0.017 ± 0.003(0.9)	0.031 ± 0.004(1.6) *	0.029 ± 0.003(1.5) *	0.025 ± 0.002(1.3) *
+ FTC 5 μM	0.017 ± 0.003(0.9)	0.037 ± 0.003(1.9) *	0.026 ± 0.002(1.4) *	0.024 ± 0.003(1.2) *
<b>Topotecan</b>	0.020 ± 0.002(1.0)	0.379 ± 0.026(18.9)	0.534 ± 0.076(26.7)	0.271 ± 0.027(13.6)
+ Cabo 2.5 μM	0.019 ± 0.006(0.9)	0.074 ± 0.005(3.7) *	0.054 ± 0.004(2.7) *	0.084 ± 0.016(4.2) *
+ Cabo 5 μM	0.017 ± 0.003(0.9)	0.027 ± 0.003(1.4) *	0.022 ± 0.003(1.1) *	0.025 ± 0.003(1.3) *
+ FTC 5 μM	0.018 ± 0.004(0.9)	0.025 ± 0.005(1.3) *	0.021 ± 0.007(1.6) *	0.021 ± 0.005(1.6) *
<b>Cisplatin</b>	2.132 ± 0.164(1.0)	2.432 ± 0.165(1.1)	2.311 ± 0.154 (1.1)	2.534 ± 0.199(1.2)
+ Cabo 2.5 μM	2.171 ± 0.152(1.0)	2.352 ± 0.174(1.1)	2.312 ± 0.321(1.1)	2.353 ± 0.232(1.1)
+ Cabo 5 μM	2.026 ± 0.171(1.0)	2.132 ± 0.154(1.0)	2.246 ± 0.354(1.1)	2.464 ± 0.253(1.1)
+ FTC 5 μM	2.113 ± 0.221(1.0)	2.143 ± 0.271(1.0)	2.312 ± 0.243(1.1)	2.432 ± 0.143(1.1)

<sup>a</sup>IC<sub>50</sub> values are represented as the mean ± standard deviation (SD).<sup>b</sup>Resistance fold was calculated by the IC<sub>50</sub> values for different substrates, and cisplatin of HEK293/pcDNA3.1 cell lines with cabozantinib or fumitremorgin C (FTC), or the resistant cell lines in the presence or absence of cabozantinib or FTC, divided by the IC<sub>50</sub> values for different substrates, and cisplatin of HEK293/pcDNA3.1 without the reversing agents.\* *P* < 0.05, versus the control group.

**Table 3**

Cabozantinib reverses ABCB1-mediated drug resistance in drug selected resistant cells

Treatment	IC <sub>50</sub> ± SD <sup>a</sup> (μM) (Resistant fold)	
	HEK293/pcDNA3.1	HEK293/ABCB1
<b>Paclitaxel</b>	0.063 ± 0.004(1.00) <sup>b</sup>	2.646 ± 0.212(42.12)
+ Cabo 2.5 μM	0.061 ± 0.003(0.96)	2.523 ± 0.232(40.19)
+ Cabo 5 μM	0.062 ± 0.006(0.97)	2.424 ± 0.233(38.47)
+ Verapamil 5 μM	0.062 ± 0.004(0.95)	0.073 ± 0.009 (0.99) <sup>*</sup>

Cell survival was determined by MTT assay as described in Material and Methods.

<sup>a</sup>IC<sub>50</sub> values are represented as the mean ± standard deviation (SD).

<sup>b</sup>Resistance fold was calculated by the IC<sub>50</sub> values for different substrates, and cisplatin of HEK293/pcDNA3.1 cell lines with cabozantinib or fumitremorgin C (FTC), or the resistant cell line HEK293/ABCB1 in the presence or absence of cabozantinib or FTC, divided by the IC<sub>50</sub> values for different substrates of HEK293/pcDNA3.1 without the reversing agents.

<sup>\*</sup>*P*<0.05, versus the control group.